Assessing impacts of sea level rise on seawater intrusion in coastal aquifers with sloped shoreline boundary

Mohammed S. Hussain and Akbar A. Javadi*

Computational Geomechanics Group, Department of Engineering, University of Exeter, North Park Road, Exeter, EX4 4QF, UK, Email: a.a.javadi@ex.ac.uk, msh218@ex.ac.uk

* Corresponding author. Tel: +44 01392263640, Fax: +44 01392217965.

Abstract:

This paper investigates the effect of gradual and instantaneous sea level rise (SLR) on the seawater intrusion (SWI) process in coastal aquifer systems with different levels of land-surface inundation. A set of hypothetical case studies with different shoreline slopes are used to conduct this numerical experiment. For the purpose of numerical modelling, a future rate of SLR from 2015 to 2100 is considered based on the moderate expectation of the Intergovernmental Panel on Climate Change (IPCC, 2001). The gradual SLR is implemented in two different stages. First, continuous and nonlinear rising of sea level is imposed starting from year 2015 up to the end of the century. After that the final value of sea level is maintained as constant in order to assess the response time spanning to a new steady state condition. The effects of pumping resulting in lowering of groundwater level are also considered together with the dynamic variation of sea level. The results show that the rate and the amount of SWI are considerably greater in aquifers with flat shoreline slopes compared with those with steep slopes. Moreover, a shorter period of time is required to reach a new steady state condition in systems with flatter slopes. The SWI process is followed by a significant depletion in quantity of freshwater resources at the end of the century. The situation is exacerbated with combined action of SLR and over-abstraction. Finally, by considering the effect of inundation of the shoreline due to gradual SLR, the sensitivity of the system to the main aquifer parameters including molecular diffusion of solute, dispersion, hydraulic conductivity and porosity is investigated.

Keywords: saltwater intrusion, sea level rise, climate change, freshwater, coastal aquifer

1. Introduction

It is generally accepted that thermal expansion of oceans and seas and melting and calving of glaciers and small ice caps (e.g., in Greenland and Antarctic) are the main consequences of the global warming leading to gradual rising of the seawater levels (IPCC, 2013; Oude Essink, 1996). Beside this, the global warming decreases the atmospheric pressure which in turn leads to increase of water level in oceans and seas. According to IPCC (2001) future SLR is expected to occur at a rate greatly exceeding that of the recent past. Sea levels have risen about 10-20 cm during the past century. By year 2100 it is expected that the rise in sea levels would be between 20 cm to 88 cm (IPCC, 2001). However, a relatively higher range (28-98 cm) of SLR has been reported by IPCC (2013) for the year 2100.

SLR has been highlighted in the literature as one of main natural factors that are negatively correlated with the hydrodynamic balance condition of aquifers in line with other natural factors (e.g. tides) and human made factors (e.g. over pumping) (Uddameri et al., 2014; Werner et al., 2013). SLR could cause problems such as impeded drainage, wetland loss (and change), erosion and inundation of the land-surface and also saltwater intrusion (Bricker, 2009; FitzGerald et al., 2008; Nicholls, 2010, 2015). These changes in ecosystem properties and processes have several direct socio-economic impacts on a wide range of sectors and issues (Nicholls, 2015; Sušnik et al., 2015). Saltwater intrusion threatens the quantity and quality of groundwater resources. Therefore, qualification of the impacts of SLR on SWI is the main focus of the present research.

During SLR, the imposed hydraulic head on the saline water body in coastal boundaries is increased. This is followed by acceleration of the lateral intrusion of seawater. According to Ghyben-Herzberg analytical relationship the effects of 1m SLR is followed by 40m reduction of freshwater thickness. In addition, overexploitation of the groundwater coupled with the

SLR has been considered as a dominant factor causing saltwater intrusion in aquifers (Bobba, 2002; Carretero et al., 2013; Langevin and Zygnerski, 2013; Loáiciga et al., 2012; Rasmussen et al., 2013; Sefelnasr and Sherif, 2014).

Sherif and Singh (1999) showed that rising of sea level by 0.5 m in the Mediterranean sea would increase the lateral intrusion of seawater by further 9 km in the Nile delta aquifer under steady condition. This finding was confirmed by Werner and Simmons (2009) by calculating 5 km of inland penetration of saline toe for the same aquifer using the sharp interface theory. On the contrary, Shrivastava (1998) notes that the lateral intrusion of seawater in a regional confined aquifer in Jamaica would be insignificant during the SLR. The insignificant SWI progress has also been reported by Abd-Elhamid and Javadi (2011) for confined aquifers. This contradictory behaviour of SWI in confined and unconfined aquifers due to SLR has been discussed by Chang et al. (2011) in detail. They argue that the lifting process of groundwater table associated with SLR is the key factor in this mechanism. Under these circumstances, the lifting of sea level in unconfined systems is followed by increasing the thickness of the saturated zone (or transmissivity) of the aquifer, which allows the saltwater wedge to penetrate further. However, the analysis of transient progress of seawater in confined aquifer has shown that there is a landward movement of the toe in the beginning followed by the reversal process until it reaches to its initial condition (Chang et al., 2011). In other words, the lifting process of groundwater would be fully offset the impacts of instantaneous SLR and thus SLR would not show any significant effects on the long term progress of the SWI. This "forward-backward" mechanism is the common trend in results of Chang et al. (2011) which are simulated under unrealistic and higher than usual rates of SLR. Watson et al. (2010) studied unconfined aquifers and introduced this "forward-backward" pattern of toe movement as "overshooting" mechanism which was also observed during the instantaneous rising of sea level.

Two different types of boundary conditions (flux controlled and head controlled boundary conditions) have been assessed by Werner and Simmons (2009), Webb and Howard (2011) and Carretero et al. (2013) in conceptual models. In the first system, the discharge of water to sea was kept constant by maintaining the seaward hydraulic gradient of the system despite rising of the sea level. For this purposes the inland head was raised to compensate the disturbance of SLR on the hydraulic gradient. Webb and Howard (2011) considered this method as the lower bound of the SWI, which is associated with minimum seawater intrusion as a result of SLR. In the second system, with upper bound strategy (head controlled system), the inland head of water was maintained despite rising of sea levels and this is associated with maximum seawater intrusion as a result of SLR.

Transient response time of different quantitative indicators of aquifer systems due to changes in sea level has been studied by a number of researchers. The response time represents the time required for each of these indictors to reach steady state condition. Kiro et al. (2008) studied the transient response time of the water table and transition zone to instantaneous and continuous drop in sea levels (SLD). Following the same principle, Watson et al. (2010) evaluated the effects of transient response time of other indicators such as submarine discharge, toe location, total mass of salt, etc, to 1 m instantaneous rise in sea level. The results concluded that the response time varies depending on the type of the indicators considered. For example in cases where the toe location is the main indicator, the response time could vary from decades to centuries while the approximate time for the water table response is about 1 decade. Chang et al. (2011) carried out a sensitivity analysis of a confined system to different parameters and showed that the system could experience a shorter response time in cases with the large values of inland freshwater flux, with small hydraulic conductivity and also in cases with high rates of the SLR.

Kooi et al. (2000) proposed an equation to assess the distance-lag between the inland migration of saltwater wedge and the shoreline during the transgression event of SLR. However, the results of their numerical experiments, simulated with 0.001 slope of the land surface, are inconsistence with the critical limit (lag index) predicated by that equation prior to numerical simulation. The implementation of relatively smaller hydrodynamic dispersion compared to molecular diffusion, in numerical simulation, has been stated by as a reason for the mentioned contradictory results (Laattoe et al., 2013). The suggested equation by Kooi et al. (2000) generally implies that under high rates of SLR, low permeability, and also low topographical slope of land, the rate of coastal transgression is faster than the lateral intrusion of saltwater. Under these circumstances the free convective density driven flow associated with the vertical mixing and fingering of salt are the common modes of the saltwater intrusion (Kooi et al., 2000; Laattoe et al., 2013).

In this paper the response of a set of hypothetical unconfined aquifers (with different sloped shorelines) to different SLR scenarios is studied. The SWI in coastal aquifers due to realistic values of projected SLR is simulated using a density dependant finite element model SUTRA code developed by Voss and Provost (2010), considering the effects of the unsaturated (vadose) zone. For the SLR scenarios, the sloped systems are first subjected to gradual rising of the sea level starting from the current steady state condition (year 2015) up to the end of the century (year 2100). Then the final value of the SLR is maintained through an extra simulation period in order to obtain new steady state condition which allows investigating the approximate response time. The effects of instantaneous rising of sea level are also investigated in sloped aquifers. Meanwhile, these sloped systems are studied under the coupled action of SLR and lowering in the inland groundwater level (e.g. due to over pumping). Finally, the roles of different hydro-physical parameters of coastal aquifer systems

on the inland encroachment of the saltwater are investigated through a sensitivity analysis, considering the effect of SLR.

2. Model Description

The base model in this study is a hypothetical unconfined aquifer with length of 1000 m and depth of 30 m. The aquifer is discretized using 2000 quadrilateral elements and 2091 nodes. It is subjected to lateral freshwater along the inland face and seawater along the sea shore boundaries. Hydrostatic pressures (heads) of h=25.6 m and h=24.0 m are used to define the freshwater and seawater boundary conditions respectively. 0.0357 is used as seawater salinity in the unit of mass fraction which is equivalent to total dissolved solids (TDS) of 35700 mg/l and chloride concentration of 19000 mg/l. Figure 1 depicts a sketch of the problem domain with the assumed boundary conditions. The aquifer is divided vertically in two layers with an unsaturated layer overlying the bottom saturated layer. The unsaturated layer has been discretized with a finer mesh in order to prevent the oscillations in the numerical outputs (Voss, 1984). In order to guarantee the spatial stability of the numerical calculations, the upper bound of the Peclet number, suggested by SUTRA, is used to define the dimensions of the FE mesh. As a rule of thumb in discretization, typical size of each finite element in horizontal direction should be less than 4αL (i.e., 4×longitudinal dispersivity) and in the vertical direction should be less than 10αT (10×transverse dispersivity). The values of αL = 5m and αT = 0.5 m are considered. Also, a molecular diffusivity of Dm= 1×10^{-9} m^2 /s is used in the numerical model. This is equivalent to the typical molecular diffusivity of NaCl at 20°C in a porous medium including tortuosity effects (Voss and Provost, 2010). Both the top and bottom layers of the aquifer are considered to be homogeneous and isotropic. The top layer represents the unsaturated zone of an unconfined flow system with permeability of 1.3 $\times10^{-12}$ m^2. The permeability of the saturated zone is 1.3×10^{-11} m^2. It is should be noted that

SUTRA uses intrinsic permeability as input parameter rather than hydraulic conductivity. The key parameter values for the groundwater flow, solute transport and porous medium are given in Table 1. In this study the Van Genuchten (1980) model is used to simulate the transient aspects of unsaturated flow in the top layer of the aquifer.

To obtain the natural initial values of pressure within the domain, first a steady state solution was obtained through an extra simulation with the above mentioned boundary conditions. The system essentially reached a steady state after 7000 time steps, with time increment of 0.25 days. The steady state conditions of the model with the sea level at 24m is assumed to represent the hydrological situation for year 2015 and it is used as the reference level for simulation of the system in the next time periods until end of the century under the action of SLR. The raising seaside boundary head is implemented in two different scenarios. In first scenario the aquifer is simulated under the more realistic rate and value of gradual SLR of 0.65m. In second scenario it is subjected to the instantaneous rising of sea level (e.g. during a tsunami). The instantaneous SLR can also be considered as limiting case of the first scenario, where the raising occurs at high rates. The results are assessed and compared for aquifers with different sloped shorelines.

3. Gradual SLR

3.1 Vertical shoreline boundary

The change in seawater level is incorporated in the simulation model by specifying time dependent boundary condition on the seaside boundary. In order to more closely replicate the rising of sea levels during the century, the model is subjected to three different increments of sea level rise starting from year 2015 up to the end of century (year 2100). An initial steady state simulation is used to estimate the current (year 2015) situation of saltwater wedge

profile in the system prior to SLR. Figure 2 shows the projected values of the global average SLR, estimated by IPCC, between 1990 and 2100 based on different economic and technological development scenarios (IPCC, 2001). The SLR values used in the present work are marked on Figure 2 for the years 2040, 2055 and 2100 which show SLR of 0.1 m, 0.2 m and 0.65 m (with respect to 2015 as the base line) respectively. The corresponding hydraulic head boundary conditions defined at the seaside in each rising period are increased linearly with time. The simulation outputs (pressure and salinity) of each time period are used as the initial condition for the next period. In this way, the nonlinear trend of SLR at the end of year 2100 is approximately captured with a series of piecewise linear functions.

Figure 3 shows the pattern of evolution of salinity distribution in the system during this head control process for the years 2015, 2055 and 2100. Under the present state the "toe" of 50% iso-concentration line (T_{50}), measured at the bottom boundary from the seaside, is located 100 m inland due to the natural hydrodynamic dispersion. The salinity wedge continues its inland intrusion to the extent that in year 2100 the T_{50} will be located at 156 m from the coast boundary.

3.2 Sloped shoreline boundary

The effect of gradual SLR on SWI in aquifers with different shoreline slopes is investigated considering the effect of the inundated land in sloping shorelines. The shoreline boundary of the base model is geometrically modified by implementing different inland slopes of 25%, 15%, 10%, 7.5% and 5% that start from elevation of 15 m above the bottom boundary (see Figure 4). The hydrostatic head at the inland and sea boundaries are maintained at 25.6 m and 24.0 m respectively. These new systems are subjected to the same likely values of SLR used in the base model. During the transgression event (SLR) prior to 2015, the seawater starts to intrude by free convection process along the inclined slopes. Progression of this density-

driven fingering of solute in vertical direction from top to bottom indicates instabilities of the aquifer flow. However, with time and as results of hydrostatic pressure imposed by seawater, and also the density gradient between freshwater and saline water, the cyclic intrusion remains the main and usually the only seen pattern of flow. During this mechanism a lot of salt is left in the aquifers by the end of year 2015.

In comparison with the base model with vertical seaside boundary, the geometrical inclination of the shoreline in the sloped models results in the loss of significant volumes of the porous medium and thus the corresponding volumes of freshwater. A flatter slope increases the overall intrusion of the saline water by providing a wider contact area of the shoreline with the seawater. The 0.5 iso-concentration profiles of the steady state conditions for year 2015 in the aquifers with different shoreline slopes are presented in Figure 4a. The values of 100 m, 141 m, 173 m, 212 m, 249 m and 314 m are calculated for the penetration of the “toe” position in these systems with vertical, 25%, 15%, 10%, 7.5% and 5% slopes respectively.

The negative effects of the inclined coastal boundaries also emerge during the rising of the mean sea level. Figures 4b and 4c (solid lines) show the variations of the same isochlor of saline/freshwater interface under gradual rising of sea level at the end of years 2055 and 2100 respectively. Generally, the additional inland penetration of the interface into these systems is about 10 to 15 m at the end of 2055 and 50-58 m at the end of the century compared to the values in 2015. Therefore the inundation of the land-surface in the sloped shorelines plays an important role in the progression of SWI. This finding is in agreement with observations reported in the literature (Ataie-Ashtiani et al., 2013; Yechieli et al., 2010).

Furthermore, the free convective fingering of salinity is not observed throughout the entire simulated models. This is consistent with the critical limit obtained from Kooi et al. (2000) 's equation. Based on the calculated values of lag index from their equation, it is predicated that

the lateral intrusion of saltwater is the dominant mode of intrusion, also in topographical slopes less than 5%.

3.3 Effects of SLR on groundwater water level

The results of variation of groundwater level during the SLR process indicate that there is a significant rise in the groundwater table. The different systems considered follow the same trend in lifting of groundwater level during SLR. In year 2100, the maximum rise in the groundwater table (corresponding to the total SLR of 0.65 m) occurs at the seaside boundary, followed by gradual declination in its value in the landward direction. This variation of the hydraulic gradient during the SLR increases the thickness of the saturated layer and reduces the submarine groundwater discharge which results in further inland penetration of the saltwater/freshwater interface (Chang et al., 2011; Katerina et al., 2013).

The results are compared with another set of numerical experiments simulated under the flux control scenario of boundary conditions. This scenario implies that the hydraulic gradient and the corresponding submarine outflow of groundwater remain constant during SLR. Accordingly, a time dependent boundary condition is used for both lateral flow regimes to account for their gradual change. By maintaining the hydraulic gradient constant at given value of 0.0016, the head profile of this scenario at the end of the century shows gradual and uniform lifting of the water table throughout the model(s); consequently the encroachment of the seawater diminishes as shown in Figure 4c (dashed lines) compared with the results illustrated for the head control scenario (solid lines).

3.4 Effects of SLR on freshwater resources

In order to highlight the vulnerability of fresh groundwater resources to contamination and the inundation of the land-surface, the total volume of the freshwater (TDS<=500 ppm) in

each aquifer is calculated as percentage of the total volume of groundwater (combined volume of all freshwater, brackish water and saline water). Figure 5 shows the quantities of freshwater in 2015 (prior to SLR) and at the end of the century (after SLR). For instance, in the system with 5% slope, the amount of freshwater in 2015 is 70.2% and the remaining 29.8% is occupied by the intrusive saline wedge which is unsuitable for potable uses (TDS>500ppm).

It is concluded from the figure that the systems with flatter slopes contain a lower quantity of freshwater in comparison to the steeper slopes. In 2100 all the aquifers show a further declination in the amount of freshwater. Again, the flatter slopes show higher levels in declinations of the freshwater storage in the aquifer compared with the others with steeper slopes. Generally the SLR causes further 5.0 to 7.0% depletion in the freshwater budget at the end of the century.

3.5 Approximate response time

To understand the long term behaviour of the aquifers beyond 2100, the developed models are subjected to an extra period of simulation by maintaining the sea level constant at 0.65 m on the seaside boundary. The time dependent variation of the overall progression of T_{50} during this combined process of SLR (gradual SLR followed by constant sea level) is illustrated in Figure 6 for all the systems. During the gradual SLR period, the response of the toe location and progress of SWI is directly related to the changes in the sea level where it follows nearly the same nonlinear trend.

The results show that during the stage when the sea level is kept constant, the further landward movement of the 0.5 isochlor is less than 0.25 m in the models with 5% and 7.5% slopes. Therefore, these aquifers are almost in steady stare conditions in the year 2100. The

other slopes experienced about 0.36 m, 0.43 m, 0.56 m and 2.1 m additional inland encroachment of the T_{50} for 10%, 15%, 25% and vertical shoreline slopes respectively. The time lag or the response time of these systems to recover a steady state condition varies from 0.4 to 2 years for slopes ranging from shallow to steep. The results suggest that the sloped shoreline accelerates the inland advancement of the saline wedge. This acceleration of the SWI process comes with increasing the total amount of intruded saline water along these slopes.

4. Instantaneous SLR scenario:

In this section the effects of instantaneous rise in sea level on SWI are investigated. Although, the instantaneous SLR is a common scenario considered in the majority of previous studies, it can be a special case of gradual rising of sea level with high (and unrealistic) rates. For this purpose another set of numerical simulations are conducted by subjecting all the aquifers to a constant and instantaneous rising of sea level by 0.65 m rather than the gradual rise considered in the previous section.

Figure7 presents the results of transient advancement of T_{50} under this (instantaneous) SLR scenario in the aquifers. The aquifers experience a new steady state condition in time period ranging from 11 to 16 years for systems ranging from low to steep slopes. At this period of time the toe locations are nearly the same as the corresponding locations obtained from the previous scenario (gradual SLR followed by constant sea level). Figure 8 compares these transient trends obtained from both scenarios of SLR in the aquifer with 10% slope.

Another important finding is that, no "overshooting" pattern (which was reported by Watson et al. (2010)) was observed in the progress of the "toe" location during the gradual or instantaneous SLR scenarios. This may be explained by the fact that in the present work more realistic values are used to represent the natural trend in SLR (based on IPCC, 2001). This

argument was also suggested by Chang et al. (2011) for supporting their findings. Another possible explanation could be that the type of inland boundary conditions adopted in this study is hydrostatic pressure head while constant flux boundary conditions were used by Watson et al. (2010). Thus, the question of the whether the type of the assumed inland boundary condition has any role in the occurrence of "overshooting" in the interface location remains a topic for future work.

5. Vulnerability of coastal aquifer system from coupled impacts of SLR and over-abstraction:

The results discussed so far have been derived from simulations under the effects of SLR as the sole factor of climate change. However in real case studies the negative impacts on SWI process are also associated with the human activities such as over-abstraction. Therefore, the combination of over-abstraction and SLR can be considered as a scenario which exacerbates the overall SWI process. To investigate this combined process, the developed systems are subjected to a gradual SLR scenario together with inland lowering of groundwater table.

It is generally known that lowering of groundwater table due to abstraction occurs at higher rates and quicker than rising of sea level. Therefore, and for simplicity, the inland piezometric head is lowered directly with a constant value of 0.5 m and all the other parameters are kept unchanged from their original values. In this case, the steady state condition (corresponding to year 2015) of all the problems with the inland head at 25.6 m is considered as initial condition.

Figure 9 shows the results of these combined processes at the end of years 2055 and 2100. The slight oscillations observed are likely to be the result of grid refinement constraints for numerical convergence. At the end of year 2055 the interface location reaches to 162 m, 198 m, 228 m, 267 m, 305 m and 372m from the sea boundary for the vertical, 25%, 15%, 10%,

7.5% and 5% sloped aquifers respectively. The interfaces continue to move inland until they reach to 238 m, 269m, 301 m, 335 m, 372 m and 443 m at the end of year 2100 for the same sloped systems respectively. Comparing the results of this combined scenario with the isolated SLR scenario indicates that the SWI is intensified by further 70-80 m advancement for T_{50} (and 90-110 m for T_{10}) of interface at the end of the century.

Figure 10 shows the transient progress of toe location during the combined scenario. At the end of year 2100 the model is subjected to an extra period of simulation by maintaining the sea level at constant value of 0.65m. The approximate times to reach equilibrium are 2.1, 2.7, 4.1, 5.5, 8.2 and 11.0 years for the 5%, 7.5%, 10%, 15%, 25% and the vertical slopes respectively. Overall, the shorelines with low slopes are the main contributor to the acceleration of SWI. The results clearly show that the SWI is sensitive to the imposed constant head lateral boundary conditions. The initial sharp increase of the inland movement of T_{50} during the first 14 years (shown in Figure 10) is attributed to new unsettled condition occurring as a result of imposed lowering of the inland water head. And after that, the impacts of inland lowering of water level are balanced and the SLR will remain as the dominant factor up to the end. The amount of the available freshwater resulted from this scenario is illustrated in the Figure 11. Comparing these results with those obtained from isolated SLR scenario (Figure 5b) suggests that this combined scenario will cause further reduction in the available storage of the freshwater in the range of about 8 to 11 %.

6. Sensitivity analysis

A parametric study is carried out to evaluate the effects of changes in different hydraulic and transport parameters, including saturated permeability, porosity, molecular diffusion of solute, and dispersivity, on the SWI process before and after gradual rising of sea level. This is done on the aquifer with 0.05-sloped shoreline. The hydrostatic heads at the inland and sea

boundaries are maintained at 25.6 m and 24.0 m respectively as in base model. A basic approach to sensitivity analysis is adopted by varying one parameter over a pre-defined range while the other parameters are kept constant. The system is simulated for the different values of this parameter to represent the current steady state condition prior to the assumed SLR (year 2015). Thereafter, the models are subjected to the same likely value of gradual SLR, up to 0.65 m until the end of year 2100 and then the sea level is assumed to remain constant. This procedure is then repeated consecutively for each of the other parameters considered in the parametric study. The 0.05 slope is deliberately chosen for this parametric study as according to Figure 6, the flow system with such slope has very short response time period and it is almost at the steady state condition at the end of the gradual SLR event in year 2100. It has been concluded from the current sensitivity analysis that the effects of all the considered parameters during the imposed constant level of sea water after year 2100 on both the SWI and the response time remain insignificant in this aquifer. Consequently, the system will experience steady state condition in year 2100 for different values of the physical parameters.

The saturated permeability of the soil is the first variable considered during the parametric study. Five different values of permeability in the range 1.3×10^{-10} m^2 to 1.3×10^{-12} m^2 are selected. The influence of permeability on the rate of the inland movement of 10%, 50% and 90% iso-concentration contours before and after gradual SLR is demonstrated in Figure 12a. In general the amount of movement of the iso-contours of the saltwater wedge is sharply increased by increasing of the permeability and then levels off at higher permeability values. In year 2015 (the initial steady state condition) the toe points of 0.5 iso-salinity lines are located at 204, 284, 314, 337 and 341 m; and in year 2100 (the steady state condition after SLR) they are at 216, 320, 372, 401 and 406 m from the coastal boundary for models with permeability values 1.3×10^{-10} m^2, 5×10^{-11} m^2,1.3×10^{-11} m^2, 5×10^{-12} m^2 and 1.3×10^{-12} m^2

respectively. In other words, between 6% and 19% of additional intrusion occurs for the considered model between the low and high permeability systems. The net SWI associated with the increase of permeability (from 1.3×10^{-10} m^2 to 1.3×10^{-12} m^2) is 137 m in year 2015 and it increases to 190 m in year 2100. So, the increasing of the permeability is responsible for additional 53 m of the net advancement of T50 at the end of the SLR event. The corresponding values for the locations of 10% and 90% iso-concentration lines (T10 and T90) are 64m and 30 m respectively.

The results of the sensitivity analysis for porosity show that a system with a relatively low porosity is more vulnerable to SWI (Figure 12 b). In year 2015 the calculated locations of T50 are 322, 318, 314, 312, 310 and 308 m from the shoreline for porosities of 0.25, 0.3, 0.35, 0.37, 0.40 and 0.45 and the corresponding values in year 2100 are 384, 380, 372, 369, 366 and 361 m. The calculated net reductions of the inland advancements of T10, T50 and T90 are 17, 9 and 7 m for increasing porosity from 0.25 to 0.45. This narrow range of variation in the amount of encroachment indicates that, to some extent, the SWI is less dependent on the porosity values of porous media.

The changing of molecular diffusion coefficient of solute (Dm) is implemented in another set of simulations by choosing five different values for Dm as 1×10^{-5}, 1×10^{-6}, 1×10^{-7}, 1×10^{-8} and 1×10^{-9} m^2/s. In the solute transport mechanism, the molecular diffusion controls spreading of solute particles along concentration gradient. For these values of Dm, the simulated toe locations of 0.5 isochlor in year 2015 are 226, 251, 298, 312 and 314 m from shoreline boundary and in year 2100 they change to 241, 271, 338, 367 and 372 m respectively (Figure 12c). The additional movement for each of the 10, 50 and 90 % iso-contours are 37, 43 and 60 m respectively. The results show that a system with higher diffusion would result in a wider thickness of mixing zone but a smaller inland encroachment of saltwater wedge. The diffusion opposes encroachment of seawater by mixing of freshwater and saline water and

consequently reducing the effect of buoyancy forces (Abarca et al., 2007). The small size of molecular diffusion coefficient of solute (Dm) means that the rate of solute transport by diffusion is usually very small relative to the rate of solute transport by advection and dispersion (Istok, 1989).

Finally, the effect of dispersivity is studied by subjecting the model to different longitudinal dispersion coefficients, αL (5m ,10m,15m, 20m and 25m) and different ratios of the transverse dispersivity to longitudinal dispersivity, αT/αL (0.05,0.07, 0.1,0.15, 0.2 and 0.25). Figure 12d shows the results of increasing of αL in the system for αT/αL equal to 0.1. By increasing the amount of αL in this range, the additional movements of T50 at the end of the century are 58, 46, 34, 31 and 25 m respectively manifesting that the systems with higher dispersivities tend to have a lower rate of the horizontal saltwater intrusion. The calculated net reduction in the movement of T50 is about 33 m at the new steady state condition (at the end of century). For T10 and T90, the net reductions are 24 and 59 m respectively. In order to represent the results for other αT/αL ratios, the net difference between the toe points of the 10 and 90 % iso-concentration lines (which is the almost equal to the thickness of the mixing zone) is used (Figures 13a and 13b). The rate of increase in the size of the mixing zone is generally reduced in cases with higher αL and αT and this reduction is more pronounced at the new steady state condition (at the end of SLR) than the current condition of the system. Increasing of both αT and αL appears to primarily affect the shape of the intrusion wedge and widen the mixing zone. The process maintains the toe of the intrusion wedge at seaside. These results are in agreement with those reported by (Abarca et al. (2007)) who showed that the width of the mixing zone at the toe of the intrusion is mainly controlled by αL while αT controls the thickness of this zone in the middle portion of the intrusion wedge.

In summary the horizontal progression of the intruding saltwater wedge due to SLR is intensified by increasing permeability and with decreasing porosity, dispersion and molecular

diffusion. The results show that the effects of variations of the first two parameters in low salinity interfaces are greater than the high salinity interfaces. In contrast, the calculated rates of reduction in the inland movement of the saltwater wedge associated with increasing the other two parameters are more remarkable in high salinity interfaces than low salinity interfaces. The increasing of both dispersion and molecular diffusion leads to increasing the width of mixing zone, even during the SLR process and consequently the intruding wedge maintains its progression in the form of spreading instead of predominant horizontal inland advancement.

7. Summary and conclusion

A comprehensive set of numerical simulations were conducted to study the effects of sea level rise on the hydrodynamics of coastal systems. For this purpose, the transient effects of instantaneous and gradual SLR on SWI were investigated in 2D unconfined aquifers with different slopes of coastal boundaries.

It has been shown that, for the aquifer systems studied, rising of sea level by 0.65m would result in further inland advancement of seawater leading to depletion in freshwater resources by about 5 to 7 % at the end of the century compared with the current situation. By considering an extra period of simulation under the constant increased sea level, the long-term effects of the process were studied in terms of the approximate time to reach a new steady sate condition after the year 2100. The results were compared with those obtained from the instantaneous SLR scenario. The calculated response time is about 0.2 to 2 years in the first approach of SLR and about 11 to 16 years in the instantaneous SLR scenario for the systems with gradients ranging from shallow to steep. The slope of the shoreline and the corresponding coastal inundation play a significant role in the progression of freshwater/saline water interface during the raising of sea level. The results also show that the

rate and the amount of the encroached seawater are significantly higher in systems with low-sloped shorelines.

The results of long-term simulations, in which the models had reached steady state condition, show almost the same amount of inland advance of saline–fresh water interface for both schemes of SLR. The effects of the lowering of the inland groundwater head (e.g., due to over abstraction) is also considered simultaneously with the SLR. Under this coupled action, the rate and amount of SWI were intensified, especially in systems with low slopes. The total calculated response time to equilibrium in this scheme is in the range of 2.1 to 11.0 years which is considerably greater than the time required for the isolated scheme of SLR (0.2 to 2 years). An implication of these findings is that the threats and the unexpected outcomes of SLR (and global warming) could have serious consequences on the quality and quantity of fresh groundwater resources, especially in shallow unconfined aquifers. The results of the parametric study also show that the inland advancement of seawater owing to the gradual SLR is aggravated by increasing the permeability and by decreasing the molecular diffusion, dispersion and porosity.

Although, assigning of SLR along the vertical face of the shoreline is a common approach that has been implemented in the literature without considering the inundation effects, the results of this numerical study highlight that ignoring of the land inundation due to SLR generally underestimates the predictions of SWI. The changes in rainfall patterns and floods, tsunamis and droughts are likely to become more common due to global warming. In order to generalize the current key findings associated with climate change, it is necessary to consider the natural effects of rainfall in numerical modelling (the surface and subsurface water interactions) simultaneously with the effects of SLR. It is generally known that groundwater recharge could help to protect the coastal aquifers against SWI. Thus reduction in groundwater recharge will increase the rate of the penetration of intruding saltwater wedge.

References

Abarca, E., Carrera, J., Sánchez-Vila, X., Dentz, M. (2007). Anisotropic dispersive Henry problem. Advances in Water Resources, 30, 913-926.

Abd-Elhamid, H., Javadi, A. (2011). Impact of sea level rise and over-pumping on seawater intrusion in coastal aquifers. Journal of Water and Climate Change, 2, 19-28.

Ataie-Ashtiani, B., Werner, A., Simmons, C., Morgan, L., Lu, C. (2013). How important is the impact of land-surface inundation on seawater intrusion caused by sea-level rise? Hydrogeol J, 21, 1673-1677.

Bobba, A.G. (2002). Numerical modelling of salt-water intrusion due to human activities and sea-level change in the Godavari Delta, India. Hydrological Sciences Journal, 47, S67-S80.

Bricker, S.H., 2009. Impacts of climate change on small island hydrology : a literature review. British Geological Survey,Groundwater Science Programme p. 21.

Carretero, S., Rapaglia, J., Bokuniewicz, H., Kruse, E. (2013). Impact of sea-level rise on saltwater intrusion length into the coastal aquifer, Partido de La Costa, Argentina. Continental Shelf Research, 61–62, 62-70.

Chang, S.W., Clement, T.P., Simpson, M.J., Lee, K.-K. (2011). Does sea-level rise have an impact on saltwater intrusion? Advances in Water Resources, 34, 1283-1291.

FitzGerald, D.M., Fenster, M.S., Argow, B.A., Buynevich, I.V. (2008). Coastal Impacts Due to Sea-Level Rise. Annual Review of Earth and Planetary Sciences, 36, 601-647.

IPCC (2001). Climate Change 2001: Impacts, Adaptation, and Vulnerability: Contribution of Working Group II to the Third Assessment Report of the Intergovernmental Panel on Climate Change, Cambridge University Press, Cambridge, UK, and New York, NY, USA.

IPCC (2013). Climate change 2013: The Physical Science Basis. Contribution of Working Group I to the Fifth Assessment Report of the Intergovernmental Panel on Climate Change, Cambridge University Press, Cambridge, United Kingdom and New York, NY, USA.

Istok, J. (1989). Groundwater Modeling by the Finite Element Method, AGU, Washington, DC.

Katerina, M., Antonis, D.K., Georgia, D. (2013). Tipping points for seawater intrusion in coastal aquifers under rising sea level. Environmental Research Letters, 8, 014001.

Kiro, Y., Yechieli, Y., Lyakhovsky, V., Shalev, E., Starinsky, A. (2008). Time response of the water table and saltwater transition zone to a base level drop. Water Resources Research, 44, W12442.

Kooi, H., Groen, J., Leijnse, A. (2000). Modes of seawater intrusion during transgressions. Water Resources Research, 36, 3581-3589.

Laattoe, T., Werner, A., Simmons, C., (2013). Seawater Intrusion Under Current Sea-Level Rise: Processes Accompanying Coastline Transgression, in: Wetzelhuetter, C. (Ed.), Groundwater in the Coastal Zones of Asia-Pacific. Springer Netherlands, pp. 295-313.

Langevin, C.D., Zygnerski, M. (2013). Effect of Sea-Level Rise on Salt Water Intrusion near a Coastal Well Field in Southeastern Florida. Groundwater, 51, 781-803.

Loáiciga, H.A., Pingel, T.J., Garcia, E.S. (2012). Sea Water Intrusion by Sea-Level Rise: Scenarios for the 21st Century. Ground Water, 50, 37-47.

Nicholls, R.J., (2010). Impacts of and Responses to Sea-Level Rise, Understanding Sea-Level Rise and Variability. Wiley-Blackwell, pp. 17-51.

Nicholls, R.J., (2015). Chapter 9 - Adapting to Sea Level Rise, in: Sherman, J.F.S.T.E.J. (Ed.), Coastal and Marine Hazards, Risks, and Disasters. Elsevier, Boston, pp. 243-270.

Oude Essink, G.H.P. (1996). Impact of sea level rise on groundwater flow regimes: A sensitivity analysis for the Netherlands.

Rasmussen, P., Sonnenborg, T.O., Goncear, G., Hinsby, K. (2013). Assessing impacts of climate change, sea level rise, and drainage canals on saltwater intrusion to coastal aquifer. Hydrol. Earth Syst. Sci., 17, 421-443.

Sefelnasr, A., Sherif, M. (2014). Impacts of Seawater Rise on Seawater Intrusion in the Nile Delta Aquifer, Egypt. Groundwater, 52, 264-276.

Sherif, M.M., Singh, V.P. (1999). Effect of climate change on sea water intrusion in coastal aquifers. Hydrological Processes, 13, 1277-1287.

Shrivastava, G. (1998). Impact of Sea Level Rise on Seawater Intrusion into Coastal Aquifer. Journal of Hydrologic Engineering, 3, 74-78.

Sušnik, J., Vamvakeridou-Lyroudia, L.S., Baumert, N., Kloos, J., Renaud, F.G., La Jeunesse, I., Mabrouk, B., Savić, D.A., Kapelan, Z., Ludwig, R., Fischer, G., Roson, R., Zografos, C.

(2015). Interdisciplinary assessment of sea-level rise and climate change impacts on the lower Nile delta, Egypt. Science of The Total Environment, 503–504, 279-288.

Uddameri, V., Singaraju, S., Hernandez, E.A. (2014). Impacts of sea-level rise and urbanization on groundwater availability and sustainability of coastal communities in semi-arid South Texas. Environ Earth Sci, 71, 2503-2515.

Van Genuchten, M.T. (1980). A closed-form equation for predicting the hydraulic conductivity of unsaturated soils. Soil Science Society of America Journal, 44, 892-898.

Voss, C.I., 1984. A finite-element simulation model for saturated-unsaturated, fluid-density-dependent ground-water flow with energy transport or chemically-reactive single-species solute transport. U.S. Geol. Surv. (USGS),Water Resour. Invest., p. 409.

Voss , C.I., Provost, A.M., 2010. SUTRA-A model for saturated-unsaturated variable-density ground-water flow with solute or energy transport. U.S. Geol. Surv. (USGS),Water Resour. Invest., p. 300.

Watson, T.A., Werner, A.D., Simmons, C.T. (2010). Transience of seawater intrusion in response to sea level rise. Water Resources Research, 46, W12533.

Webb, M.D., Howard, K.W.F. (2011). Modeling the Transient Response of Saline Intrusion to Rising Sea-Levels. Ground Water, 49, 560-569.

Werner, A.D., Bakker, M., Post, V.E.A., Vandenbohede, A., Lu, C., Ataie-Ashtiani, B., Simmons, C.T., Barry, D.A. (2013). Seawater intrusion processes, investigation and management: Recent advances and future challenges. Advances in Water Resources, 51, 3-26.

Werner, A.D., Simmons, C.T. (2009). Impact of Sea-Level Rise on Sea Water Intrusion in Coastal Aquifers. Ground Water, 47, 197-204.

Yechieli, Y., Shalev, E., Wollman, S., Kiro, Y., Kafri, U. (2010). Response of the Mediterranean and Dead Sea coastal aquifers to sea level variations. Water Resources Research, 46, W12550.

List of Figures:

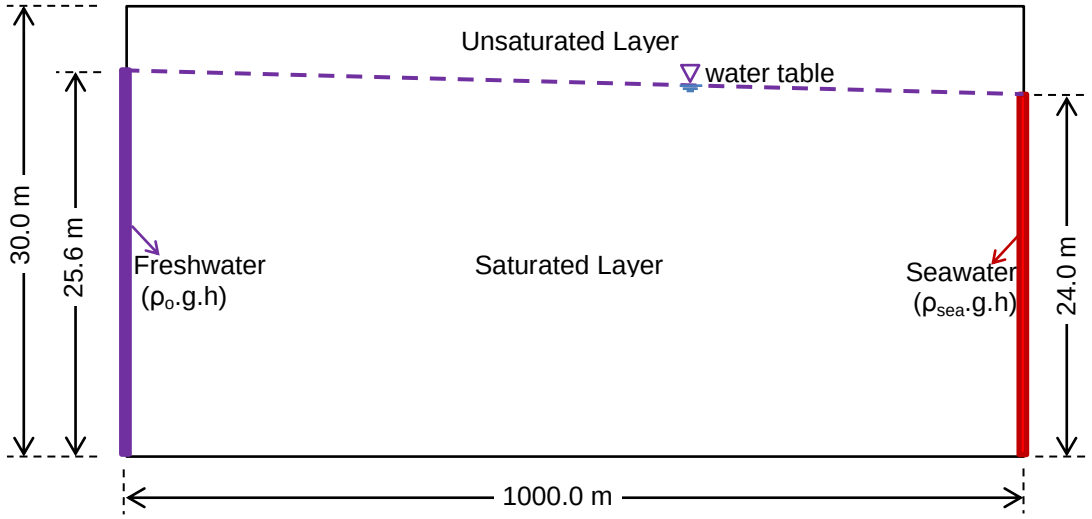

Figure 1: The base model and boundary conditions

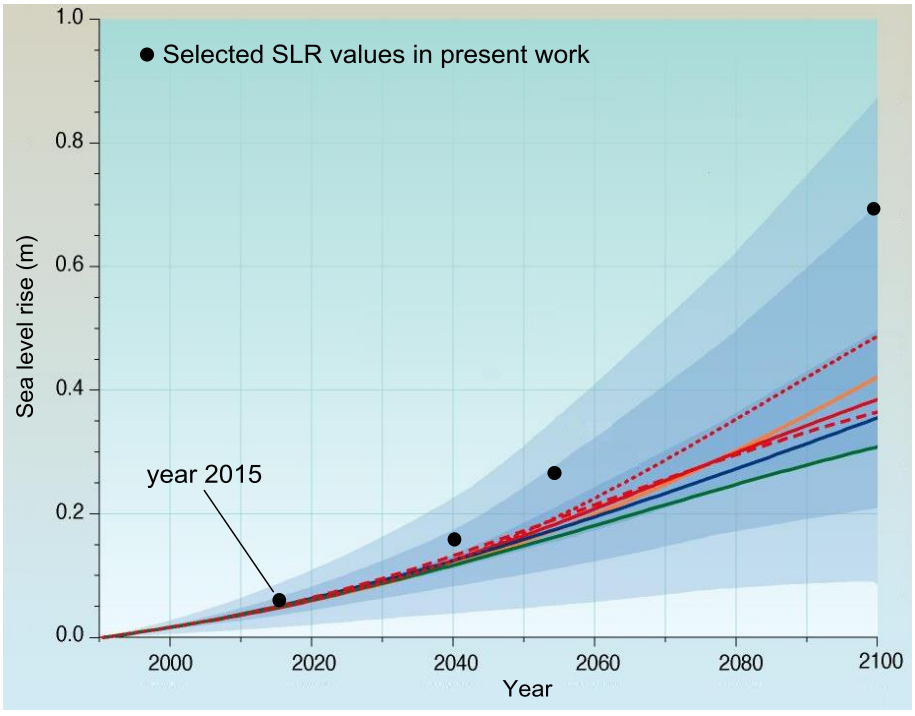

Figure 2: Global average SLR estimated by IPCC (2001)

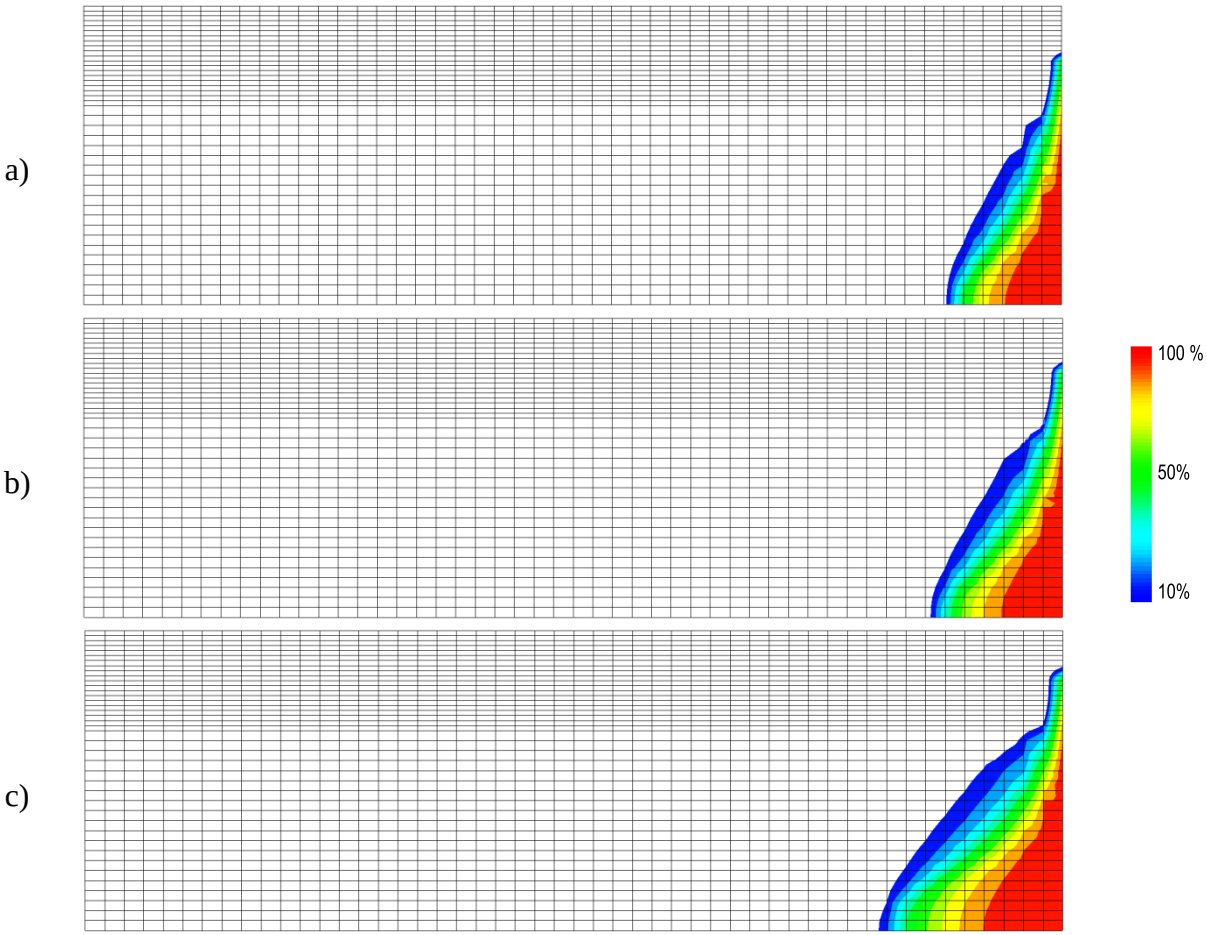

Figure 3: Salinity distribution prior the SLR a) year 2015; and during the SLR in b) year 2055; c) year 2100

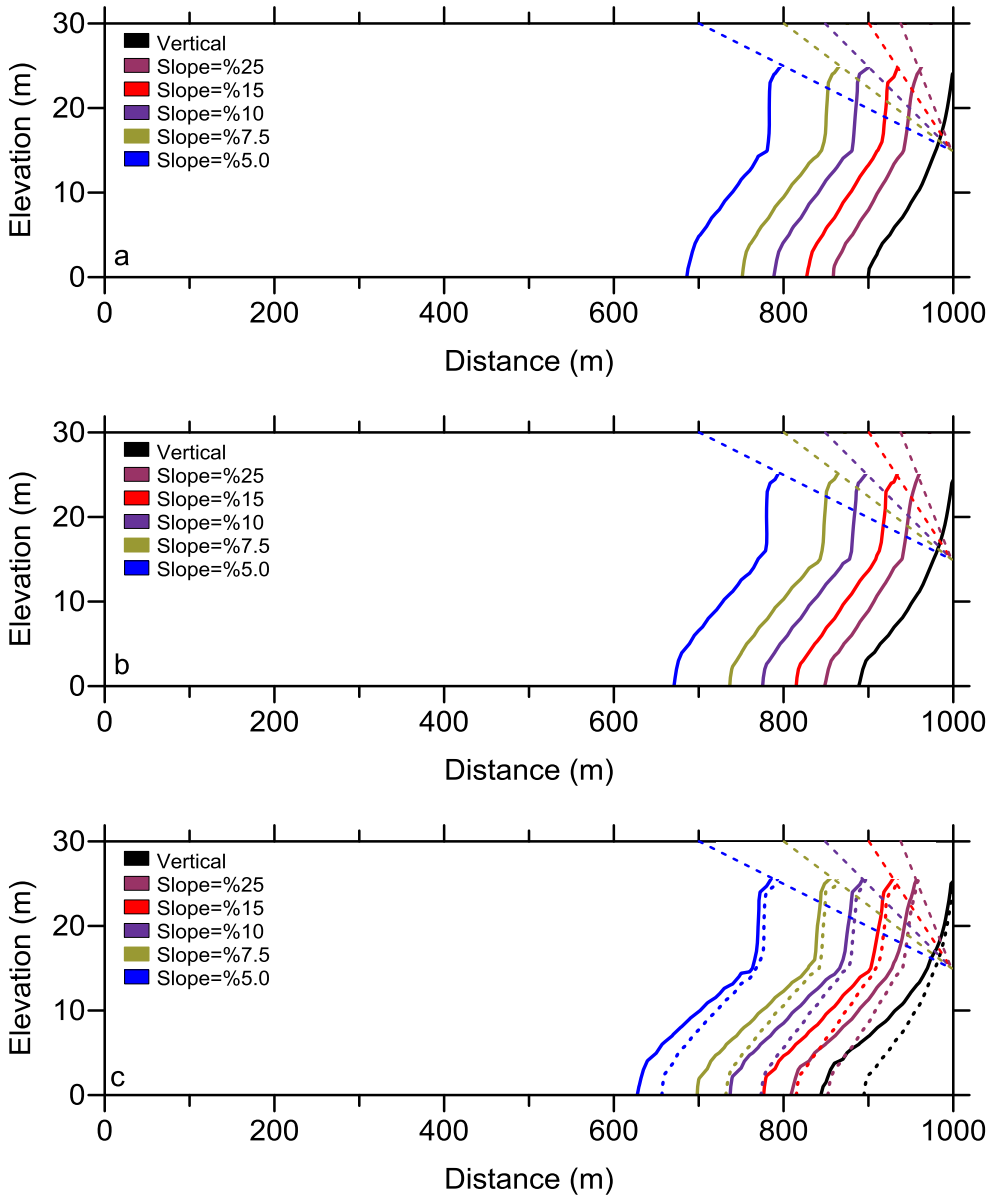

Figure 4: a) Steady state positions of 50% iso-concentration lines of SWI in the aquifers with different coastal slopes in (a) year 2015; (b) year 2055 and (c) year 2100, head control (solid lines) and flux control (dashed lines) scenarios.

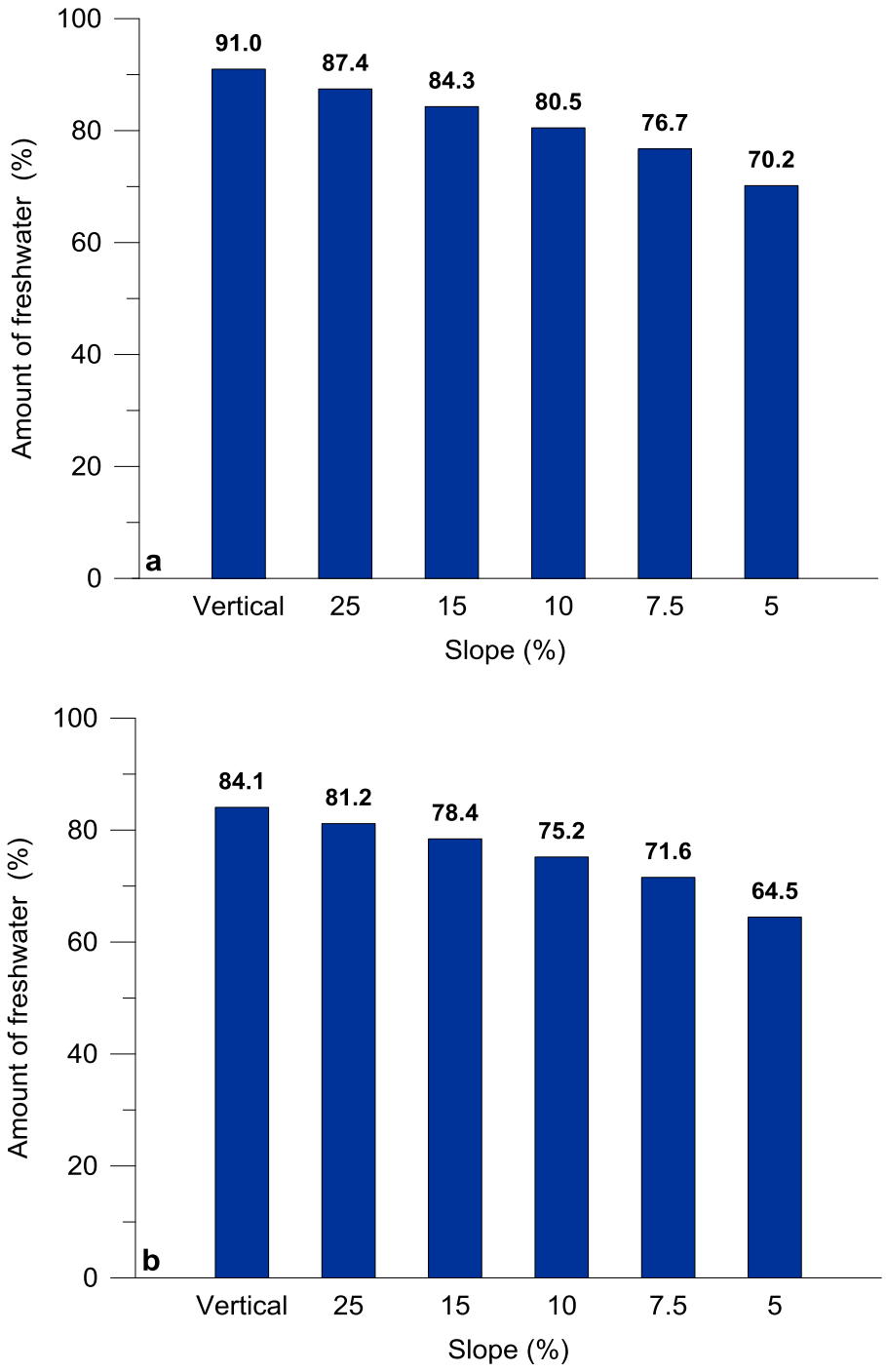

Figure 5: Total amount of freshwater storage (%) in (a) year 2015 and (b) year 2100

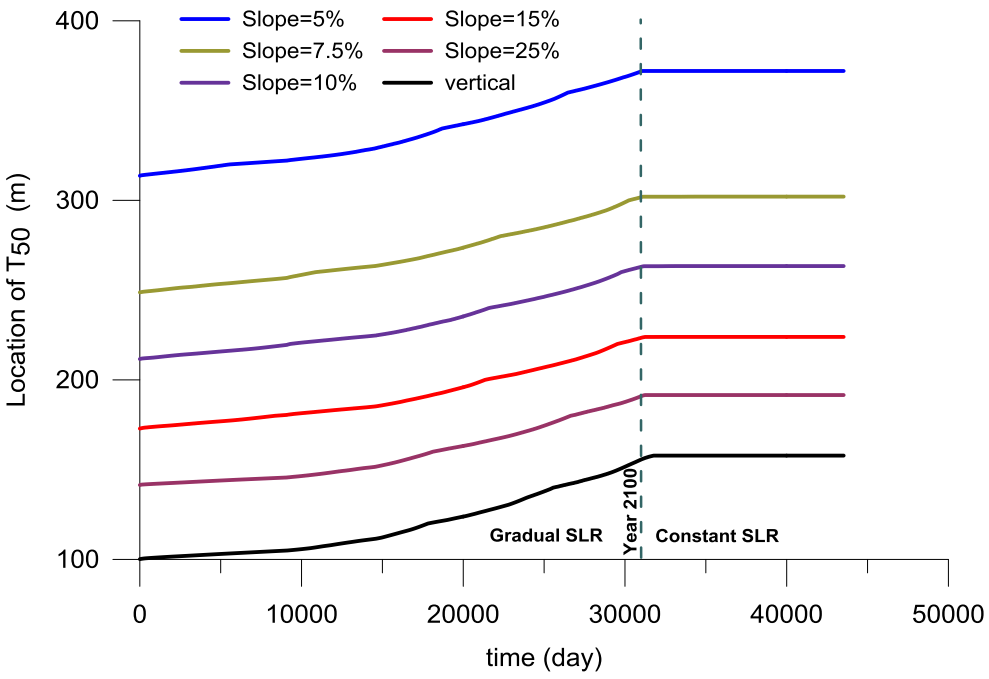

Figure 6: Transient inland progression of the toe location (T_{50}) during the combined (gradual and constant) scenario of the SLR

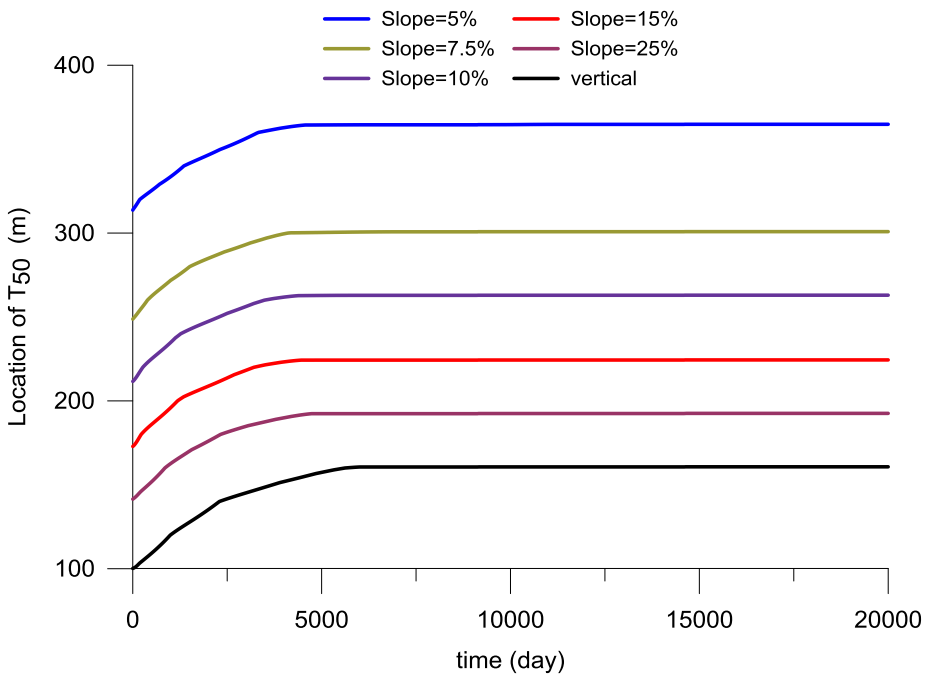

Figure 7: Inland advancement of the toe location (T_{50}) during the direct SLR scenario

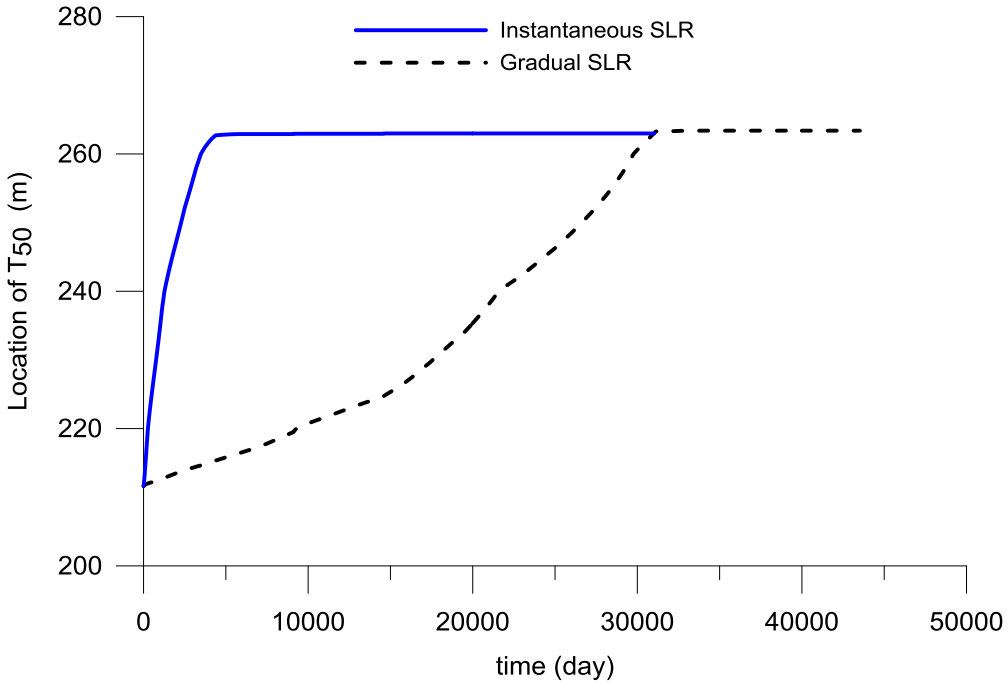

Figure 8: Comparison of the inland advancement of T_{50} during the direct SLR and gradual SLR scenarios in aquifer with 10% shoreline slope

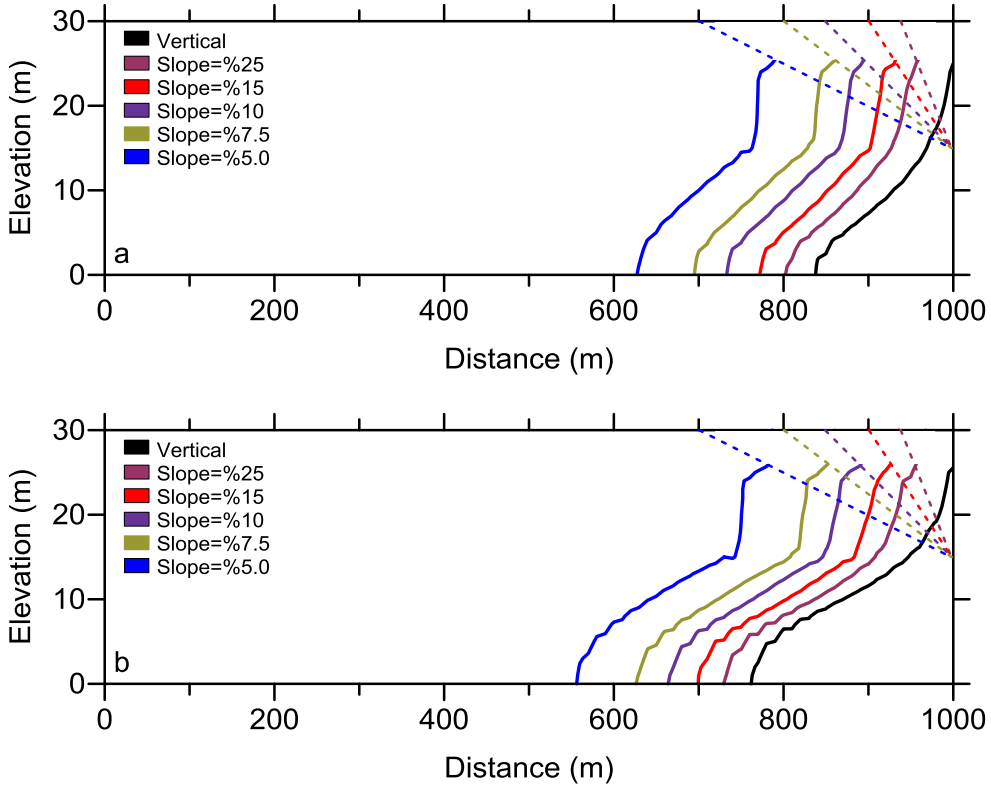

Figure 9: Variations of 50% iso-concentration lines of SWI under the impacts of combined SLR and lowering of the inland water level in (a) year 2055 and (b) year 2100

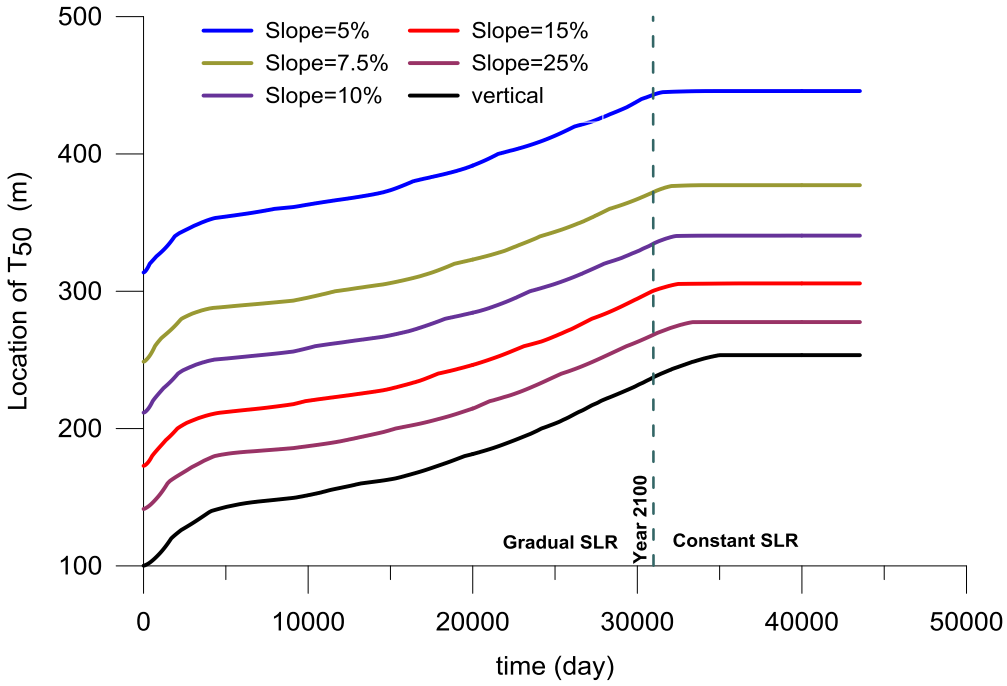

Figure 10: Inland progressing of the toe location (T_{50}) during the combined (SLR and lowering of the inland head) scenario

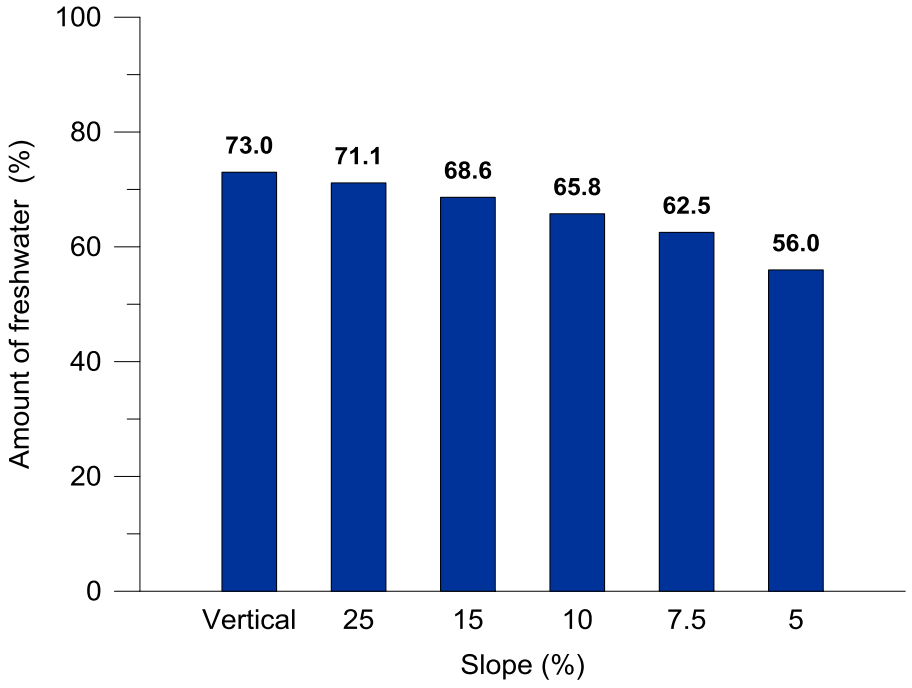

Figure 11: Total amount of freshwater storage (%) during the combined (SLR and lowering of the inland head) scenario in year 2015

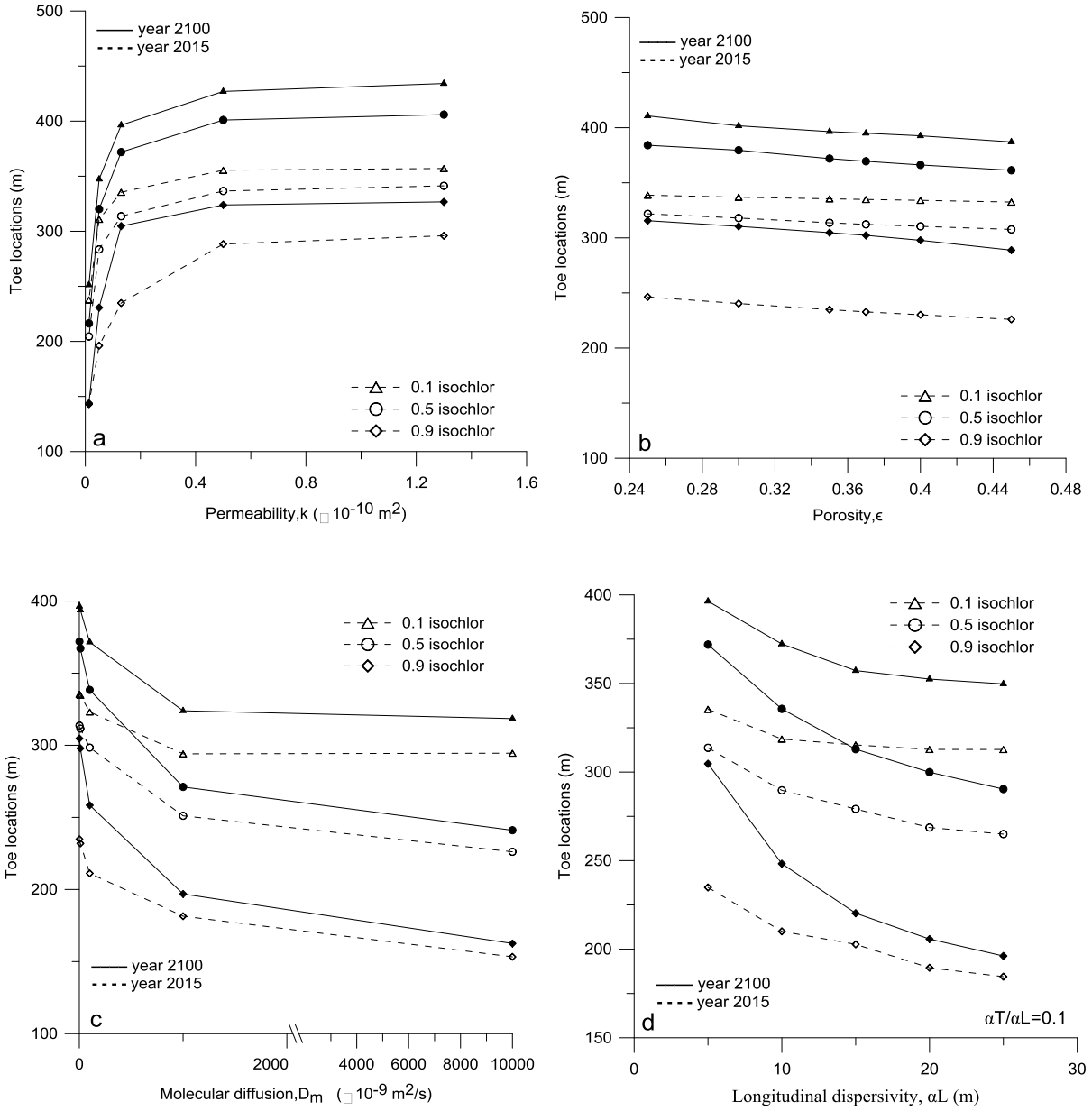

Figure 12: Variations of toe locations as distance from the shoreline boundary with (a) permeability; (b) porosity; (c) molecular diffusion coefficient and (d) longitudinal dispersivity calculated at the initial (year 2015) and final steady state conditions (in year 2100 after SLR)

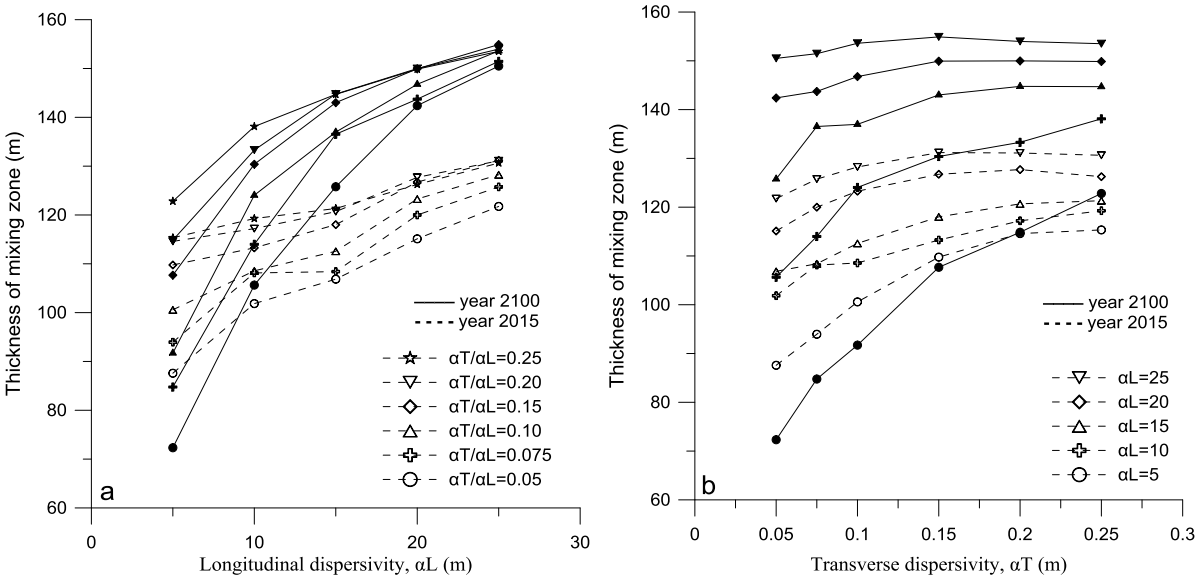

Figure 13: Variations of the mixing zone thickness with (a) longitudinal dispersivity and (b) transverse dispersivity obtained at the initial (prior to SLR) and final steady state conditions (after SLR)